

Proof-of-Concept MARG-Based Glove for Intuitive 3D Human-Computer Interaction

Pontakorn Sonchan^(⊠), Neeranut Ratchatanantakit, Nonnarit O-larnnithipong, Malek Adjouadi, and Armando Barreto

Department of Electrical and Computer Engineering, Florida International University, Miami, FL, USA

{psonc001,nratc001,nolarnni,adjouadi,barretoa}@fiu.edu

Abstract. Numerous applications of Virtual Reality (VR) and Augmented Reality (AR) continue to emerge. However, many of the current mechanisms to provide input in those environments still require the user to perform actions (e.g., press a number of buttons, tilt a stick) that are not natural or intuitive. It would be desirable to enable users of 3D virtual environments to use natural hand gestures to interact with the environments. The implementation of a glove capable of tracking the movement and configuration of a user's hand has been pursued by multiple groups in the past. One of the most recent approaches consists of tracking the motion of the hand and fingers using miniature sensor modules with magnetic and inertial sensors. Unfortunately, the limited quality of the signals from those sensors and the frequent deviation from the assumptions made in the design of their operations have prevented the implementation of a tracking glove able to achieve high performance and large-scale acceptance. This paper describes our development of a proof-of-concept glove that incorporates motion sensors and a signal processing algorithm designed to maintain high tracking performance even in locations that are challenging to these sensors, (e.g., where the geomagnetic field is distorted by nearby ferromagnetic objects). We describe the integration of the required components, the rationale and outline of the tracking algorithms and the virtual reality environment in which the tracking results drive the movements of the model of a hand. We also describe the protocol that will be used to evaluate the performance of the glove.

Keywords: MARG module \cdot Orientation Estimation \cdot Magnetic Disturbance \cdot Hand Tracking Glove

1 Motivation

1.1 Limitations of Traditional Hardware Input Devices

Applications of Virtual Reality (VR) and Augmented Reality (AR) continue to rapidly emerge in multiple industries. For example, important applications of VR and AR have been found in the education, sports, and military arenas [3, 13, 16]. This hardware and software technology allows humans to execute tasks in virtual spaces through their

actions in physical space, for entertainment or training purposes. However, the potential for convincing user immersion in VR and AR environments is degraded by the kind of input devices used, which could be mere adaptations of legacy 2-D controllers. Controllers, such as the mouse, allow a user to control the computer in a 2D virtual space. However, those traditional controllers are not fully adequate to maximize the potential of working with a 3D virtual environment. Even though there have been new hardware developments for modern 3D simulation such as the Wii Mote or a variety of VR remote controllers (such as HTC's Vive, Oculus Quest hand controller, etc.), they do not provide the user with a full hand control experience. Even in some of the newest VR systems, such as the Meta Quest 3 and the PlayStation VR2 the input devices are non-anthropomorphic hand-held devices. These devices require the user to provide input to the system by pressing a few buttons in the device.

In this context, several groups have pursued the development of a glove that could track the position and configuration of the user hand [5, 11], allowing for the use of more natural and intuitive hand gestures and micro gestures to provide input to the VR and AR systems. Several attempts to the development of such glove have used Magnetic, Angular-Rate and Gravity (MARG) sensor modules as their main sensing devices. However, the limited accuracy of this Micro Electro-Mechanical System (MEMS) sensors has challenged the successful implementation of the glove, with particular vulnerabilities in environments where the magnetic field is not uniform (possibly due to the pervasive presence of ferromagnetic objects) [4, 18]. In this paper we present the development of a proof-of concept implementation of a proposed human-computer interaction glove which employs our custom processing algorithm to obtain the orientations of the MARG modules embedded in the glove.

2 System Design and Hardware Components

The human-computer interaction glove we seek must have the ability to track the position and configuration (orientation of articulated segments) of the user's hand in real time. Our glove pursues that goal on the basis of the hardware components described in Sects. 2.1 and 2.2, the virtual reality interpretation of the glove signals described in Sect. 2.3, and the custom orientation estimation algorithm outlined in Sect. 3.

2.1 A MARG-Based Glove

There are now in the market multiple miniature Magnetic, Angular-Rate, Gravity (MARG) sensor modules, which are small, lightweight and low-power. These characteristics of MARG modules have inspired multiple groups to attach them to diverse articulated segments of the body, such as the fingers, to track their orientation. Each of these MARG modules comprises:

- Tri-axial gyroscopes which track the angular change rate (ω) of the module.
- *Tri-axial accelerometers* which, if the MARG is static, sense only the gravity vector. If there is linear acceleration applied to the module, the accelerometer responds to the superposition of those 2 vectors.

• *Tri-axial magnetometers* meant to measure the geomagnetic vector, which points to the magnetic north.

If the MARG is properly attached to an articulated segment of the body (e.g., a phalanx in the hand), the signals provided by the MARG are processed by a controller to estimate the MARG orientation (and, by extension, the orientation of the articulated segment), in real time. An initial estimate of the orientation can be obtained by integration of the angular velocities reported by the gyroscope in the MARG to the controller. However, this initial estimation of the orientation of a MARG must frequently be corrected, since even small offsets commonly included in the outputs of consumer-grade MEMS gyroscopes [1] will produce increasing orientation errors ("drift") when they are integrated [2, 6, 21]. This significantly challenges the use of MEMS MARG modules for hand tracking, in the context of human-computer interaction, with several of the devices previously developed confined to mainly clinical applications, in restricted use environments.

We propose the development of a glove instrumented with one MARG in the dorsal surface of the hand and two of them in each finger (proximal and middle phalanges), except for the thumb, which is tracked with three modules. We utilize the Yost Labs 3-Space Nano MARG modules [23] in their carrier printed circuit boards ($16 \times 17 \times 1.7$ mm, 0.9 g). Signals from all the MARG modules are collected by a controller, also placed in the dorsal region of the hand, and are then transmitted wirelessly to the computer system. The proposed placement of the MARG modules is shown in Fig. 1.



Fig. 1. Conceptual depiction of the glove, indicating the placement of the MARG modules. In the first proof-of-concept implementation two MARG modules are used to instrument the middle finger, two for the index finger and three for the thumb, in addition to the module placed on the dorsal surface of the glove.

For a first proof-of-concept prototype we have placed a total eight sensors attached to the outside of the glove to track the orientation of the dorsal surface of the metacarpal

mass, the thumb and the index and middle fingers (exclusively). The proposed placement of the sensors in the prototype is shown in Fig. 2.

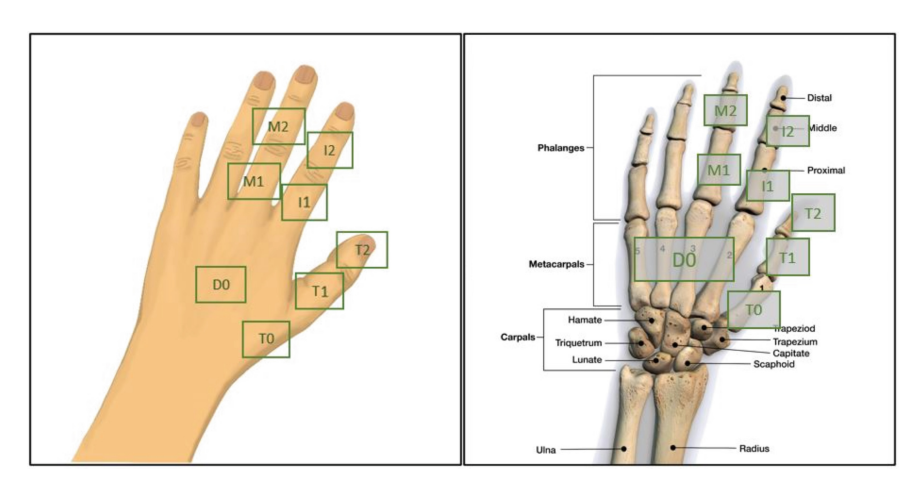


Fig. 2. Correspondence between the bone structure of the hand and the proposed placement of MARG modules for the prototype glove (Right pane is modified from an iStock image, www.ist ockphoto.com, used with permission).

The D0 sensor is placed on the dorsal surface of the glove to track the orientation of the metacarpal mass, i.e., the volume occupied by the 2nd, 3rd, 4th and 5th metacarpals, which we are considering as a single rigid body. Therefore, the signals from D0 are used to track what would normally be described as the "orientation of the palm", or less precisely "the orientation of the hand" (which disregards the orientations of the fingers).

To track movement of the middle finger, there are two modules on the glove. Sensor M1 is attached on the proximal phalanx of the middle finger. The second segment of the middle finger is its middle phalanx, and sensor M2 is placed at this location. Similarly, tracking the orientation of the segments of the index finger is accomplished by using two modules, I1 and I2, attached to the index finger's proximal phalanx and middle phalanx, respectively.

On the thumb, which is different from those two fingers, the glove needs three sensors to be able to track all the possible movements. Because the thumb metacarpal is articulated, sensor T0 is dedicated to tracking this segment. Sensor T1 tracks the proximal phalanx. Since the thumb does not have the middle phalanx, sensor T2 is tracking the distal phalanx.

We have not attempted to attach MARG sensors on the distal phalanges of the index and middle fingers because the joint between the middle and distal phalanges of these fingers has only one degree of freedom (like a door hinge), so that the distal phalanx can only turn in the plane in which the middle phalanx lies. Furthermore, the angle by which the distal phalanx turns (with respect to the middle phalanx), θ_{Distal} , is proportional to the angle by which the middle phalanx turns (with respect to the proximal phalanx),

 θ_{Middle} , according to Eq. 1, reproduced from [9].

$$\theta_{Distal} = \frac{2}{3} \theta_{Middle} \tag{1}$$

Table 1 summarizes how the orientation of the segments tracked is measured or calculated.

Finger	Phalanges*	Sensor ID	Tracker
Dorsal	Dorsal	D0	MARG Module
Middle Finger	Proximal	M1	MARG Module
	Middle	M2	MARG Module
	Distal	-	Calculation
Index Finger	Proximal	I1	MARG Module
	Middle	I2	MARG Module
	Distal	-	Calculation
Thumb	*Metacarpal	T0	MARG Module
	Proximal	T1	MARG Module
	Distal	T2	MARG Module

Table 1. Measurement/calculation of the orientation of hand segments

2.2 RGB-D Camera and Nuitrack Software Development Kit (Nuitrack SDK)

The second hardware component of our system is the RGB-D camera used to obtain the spatial position of the hand in real time. We model each finger as a kinematic chain that includes the metacarpal mass and the phalanges of that finger, whose lengths can be measured in advance. Accordingly, instantaneous knowledge of the 3D position of just the wrist end of the metacarpal mass and the orientation of all the segments of the chain allows the determination of the 3D positions of all the joints in the chain. We have used the commercially available Intel® RealSenseTM Depth Camera D455 [8] in conjunction with the Nuitrack SDK [17] to track the 3D coordinates of the wrist. This is a low-cost camera of compact size ($124 \times 29 \times 26$ mm) which is, therefore, suitable for operating in a general working space, for example, a desk with a personal computer. The D455 camera can be connected to the system by using a USB 3 cable. The recommended distance range for the D455 camera is from 60 cm to 600 cm, which should be appropriate for a variety of prospective VR or AR use cases.

The Nuitrack SDK uses machine learning techniques to perform skeleton tracking, aiming at the identification of the shape of a human in the frame and yielding estimates of the X, Y, Z positions of the major joints of the body, including both wrists. Because the system seeks the tracking of the complete skeleton, it is less susceptible to disruptions in the wrist location recognition due to partial occlusion of the arm of the user, making this approach to position tracking a robust one (Fig. 3).

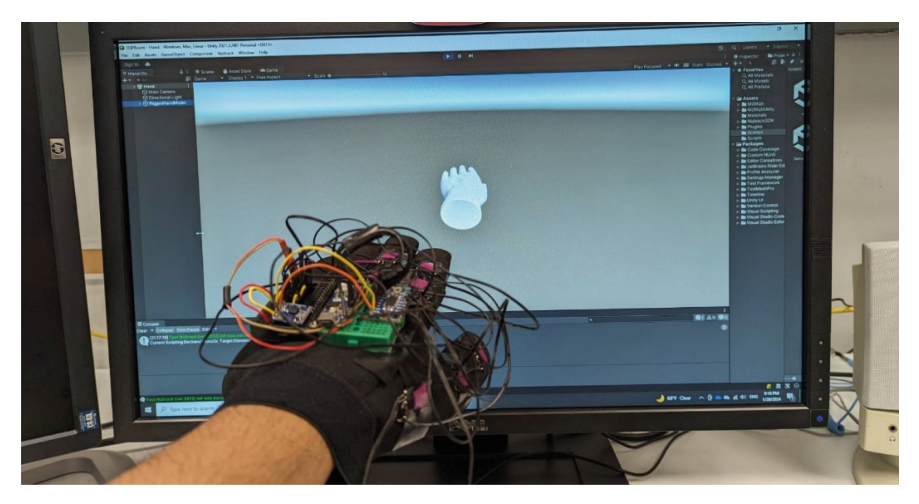


Fig. 3. Proof-of-concept prototype glove (The discrete circuit boards placed on the dorsal surface of the glove could eventually be consolidated in a single chip).

2.3 Virtual Environment Simulation

The third element in our development of the glove interface is the virtual hand representation that moves in response to the movements performed in the physical world by the user who wears the glove. The virtual hand is represented in a virtual working space developed within Unity®, the game engine that provides 3D development tools, including the creation and manipulation of basic 3D components (cube, sphere, plane, etc.) in the development environment. The components in Unity® can be animated by using the C# programming language (scripting with the MonoBehavior API). For our project, a virtual hand model was defined and the position of the hand in the virtual environment is determined by the 3D wrist coordinates obtained from the Nuitrack SDK. Simultaneously, the articulated segments of the virtual hand are oriented according to the orientation estimates defined from the signals of each corresponding MARG module.

One of the key objectives of the procedure designed to evaluate the prototype (detailed in Sect. 4) is the study of its robustness with respect to the potential magnetic field distortions present in the physical operating environment of the glove due to the presence of ferromagnetic objects within it. Accordingly, virtual 3D targets (cubes) were placed in regions of the virtual environment that correspond to physical regions with and without magnetic distortions.

Figure 4 shows the 3D simulation of the experiment where the user will perform an evaluation task. The user will visualize the virtual scenario including the virtual hand controlled by the glove and a number of cubic targets. The user will then be asked to reach to and "acquire" the targets by simultaneously touching the top and bottom surfaces of the virtual cubes.

The three green cubes shown on the left section of Fig. 4 have virtual placements that match locations in the physical world where the geomagnetic filed is not distorted. In contrast, the three orange cubes shown on the right section of Fig. 4 have virtual placements that match physical world locations where the geomagnetic field will be

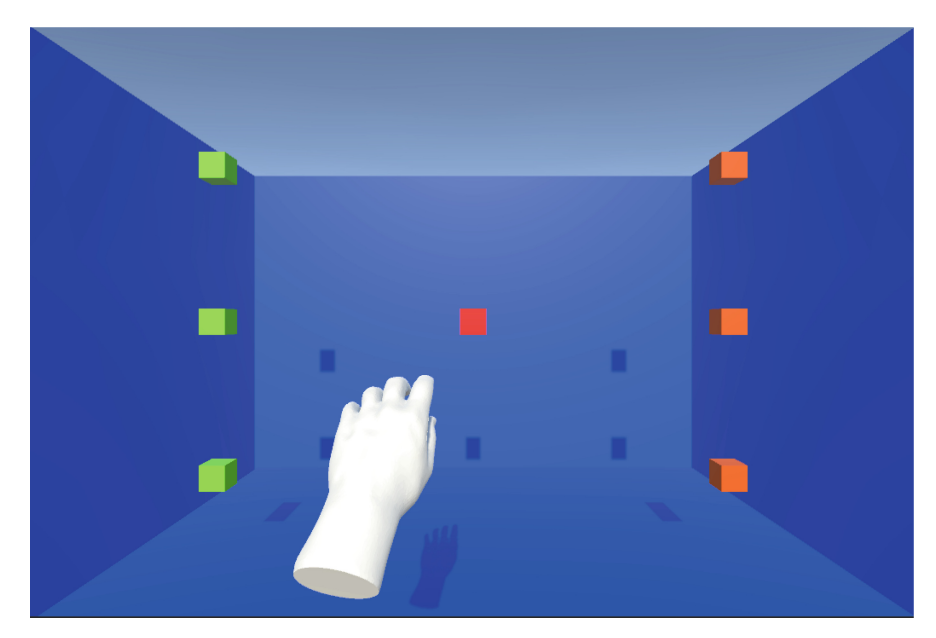


Fig. 4. The 3D simulation for a user to perform the evaluation experiment.

distorted by the placement of ferromagnetic bars of high magnetic permeability (M35 HSS high speed steel). This setup will allow the comparison of system performance under both types of condition: with and without magnetic distortions, which is one of the important objectives of the evaluation.

When the users move their hand in the physical space, the D455 camera and Nuitrack SDK will report the sequence of X, Y, and Z coordinates traveled by the subject's wrist. In response, the position of the virtual hand will be updated accordingly in the simulation.

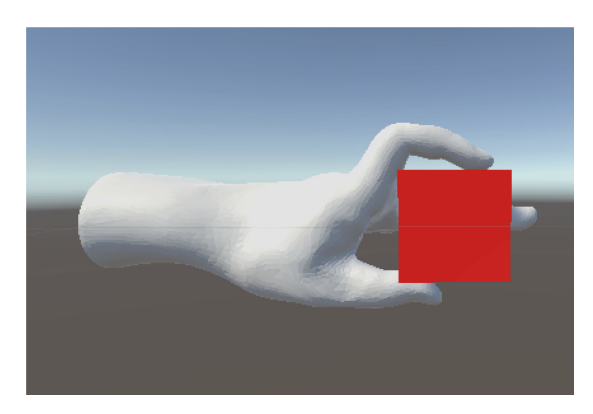


Fig. 5. A user must touch the top and the bottom of the virtual target with the index finger and thumb for target acquisition

The user can move the 3D hand model freely as long as the hand in the physical world is still within in the camera's view.

Figure 5 exemplifies the hand actions required for the completion of a successful cube "acquisition" in the system. The index finger of the 3D model must touch the top surface of a cube while, simultaneously, the thumb must touch the bottom surface of the cube.

3 MARG Orientation Estimation Algorithm, the Gravity and North Vector-Double SLERP with μ_k (GMVD μk)

The efficacy of the system described in the preceding sections depends critically on the correctness of the orientation estimates obtained for each articulated hand segment from the gyroscope, accelerometer and magnetometer signals output by the corresponding MARG modules. While there have been numerous algorithms proposed for this type of MARG orientation estimation [14, 15], we use our Gravity and North Vector – Double SLERP with μ_k (GMVD μk) algorithm [19]. The algorithm seeks to judiciously combine all available readings from the MARG module, to obtain a final orientation estimate. This approach systematically selects the level of involvement of each sensor type after assessing their trustworthiness parameters. These trustworthiness parameters reflect the instantaneous characteristics of the sensor's environment. If the instantaneous MARG conditions diverge significantly from the assumptions made pertaining the use of accelerometer or magnetometer data to enrich the orientation estimate, then the corresponding sensor information will not be involved strongly in the definition of the final orientation estimate. That is, GMVDµk implements a form of conditional involvement of the available information sources. The following sections outline how this goal is achieved. For a more detailed description of the algorithm, the reader is referred to [19].

3.1 Information Flow in the GMVDµk Algorithm

At the beginning of each iteration of the algorithm, the latest raw data of gyroscope readings, ω , accelerometer readings, a_0 , and magnetometer readings, m_0 , will be read. (In this algorithm description vector quantities are represented by bold symbols.) The readings from the gyroscope, ω , will be "de-biased" by subtracting from them dynamic estimates of the most recent levels of bias. It is known, however, that processes like this have only limited effectiveness in removing bias levels, therefore, the rest of the processing steps described here become necessary. The "de-biased" gyroscope signals, denoted ω_B , are used for the rest of the iteration.

GMVD μ k represents orientations as quaternions [7, 12, 20] (which will also be represented by bold symbols). An initial orientation estimation is represented in quaternion form as q_G . In each iteration, q_G can be established by recursive integration of the gyroscope's readings, as indicated in Eqs. 2 and 3. In these equations \dot{q} is "quaternion rate of change" that is computed from ω_B and q_0 , which is the quaternion representing the orientation resulting from the previous iteration. In Eq. 2 the symbol \otimes represents quaternion multiplication. In Eq. 3, the rate of change is integrated (accumulated) to

represent a first estimation of the current orientation quaternion, q_G , where Δt is the sampling interval and q_0^* is the quaternion conjugate of q_0 .

$$\dot{q} = \frac{1}{2}q_0 \otimes \omega_B \tag{2}$$

$$\mathbf{q}_G = e^{\left((\Delta t)\dot{\mathbf{q}}\otimes\mathbf{q}_0^*\right)}\otimes\mathbf{q}_0 \tag{3}$$

Now the algorithm has an initial quaternion representing the orientation of the MARG. However, unavoidable offset remnants in the gyroscope signals, $\omega_{\rm B}$, will gradually introduce "drift" in the $q_{\rm G}$ estimate obtained from rotational speed integration alone. Thus, a correction of this initial estimate, leveraging the information contained in the accelerometer and magnetometer signals, is implemented next. In fact, our approach implements two parallel processes to correct $q_{\rm G}$ using accelerometer information and magnetometer information, but restraining their relative correction weights when the corresponding assumptions are not fully met. For the sake of brevity only the process that yields the accelerometer-corrected version of $q_{\rm G}$, designated by $q_{\rm SA}$, will be outlined here, noting that the generation of the magnetometer-corrected version, $q_{\rm SM}$, is analogous and is further detailed in [19].

When the MARG is static (or nearly static) the accelerometer's real-time readings, a_0 , point in the direction of the gravitational vector (perpendicular to the floor, pointing downwards). On the other hand, Eq. 4 shows how an initial measurement of the gravitational vector, A_{INIT} , acquired during the system startup (while the MARG was at its reference orientation), is mapped to the current orientation of the MARG body frame. The resulting $a(q_G)$ is a "computed" version of the current accelerometer readings.

$$a(q_G) = q_G^* \otimes A_{INIT} \otimes q_G \tag{4}$$

If the initial estimate q_G were not affected by drift these body frame-referenced directions should match. In practice, however, we assume there might be a distortion already present in q_G , which produces a "quaternion difference" between the calculated version and the measured version of the instantaneous accelerometer readings. We express this orientation difference as a quaternion, Δq_A , (the A-subscript stands for Accelerometer) by calculating its vector part (Eq. 5) and its scalar part (Eq. 6), and then fusing them into the difference quaternion (Eq. 7), with the "H operator".

$$\mathbf{q}_{Av} = \mathbf{a}_0 \times \mathbf{a}(\mathbf{q}_G) \tag{5}$$

$$q_{Aw} = ||a_0|| ||a(q_G)|| + a_0 \cdot a(q_G)$$
(6)

$$\Delta q_A = H(q_{Av}, q_{Aw}) \tag{7}$$

This Δq_A is, in fact, the supplementary rotation that would be needed to make the computed $a(q_G)$ match with the measured a_0 . Equivalently, the two vectors would also match if Δq_A were to be "compounded" with the original q_G , to yield a fully-accelerometer-corrected quaternion q_{GA} as indicated in Eq. 8.

$$q_{GA} = q_G \otimes \Delta q_A \tag{8}$$

In a parallel track of processing, a fully-magnetometer-corrected orientation estimate, $q_{\rm GM}$, is obtained by implementation of equations similar to Eqs. 4–8, which operate with the magnetic counterparts to the accelerometer concepts cited above $(M_{\rm INIT}, m_0, m(q_{\rm G}), {\rm etc.})$.

Since the appropriateness of the accelerometer- and magnetometer-based corrections are predicated on the fulfillment of specific assumptions (e.g., that the local geomagnetic field is undistorted), our algorithm uses Spherical Linear Interpolation (SLERP), to defined partially-corrected quaternions where the strength of the corresponding correction has been restricted in proportion to the values of accelerometer and magnetometer trustworthiness parameters ($0 \le \alpha \le 1$ and $0 \le \mu \le 1$), assessed by the algorithm for every iteration. The partially accelerometer- and magnetometer-corrected orientation estimates, q_{SA} and q_{SM} , respectively, are therefore computed as indicated in Eq. 9 and Eq. 10.

$$\mathbf{q}_{SA} = SLERP(\mathbf{q}_G, \mathbf{q}_{GA}, \alpha) \tag{9}$$

$$\mathbf{q}_{SM} = SLERP(\mathbf{q}_G, \mathbf{q}_{GM}, \mu) \tag{10}$$

Each one of these equations represents the use of SLERP to interpolate a quaternion from q_G to a second quaternion (q_{GA} or q_{GM}) under control of the third parameter. So, for example, if alpha is close to zero, q_{SA} will be close to q_G (minimal correction from accelerometer information), whereas if alpha is close to one, q_{SA} will be close to q_{GA} (close to full correction based of accelerometer information). Finally, q_{SA} and q_{SM} are fused through a second tier of SLERP interpolation, controlled by alpha, at the end of each iteration to obtain the final orientation estimate quaternion q_{OUT} , as indicated in Eq. 11. This q_{OUT} is the effective result of each orientation estimation iteration, to be utilized by external orientation tracking applications.

$$\mathbf{q}_{OUT} = SLERP(\mathbf{q}_{SM}, \mathbf{q}_{SA}, \alpha) \tag{11}$$

Additionally, this $q_{\rm OUT}$ is the "previous orientation" considered at the beginning of the next iteration of the correction process, as mentioned in Eqs. 2 and 3. Equation 12 shows the relation between q_0 and $q_{\rm OUT}$.

$$\mathbf{q}_0 = \begin{cases} [0001], & iteration = 1\\ \mathbf{q}_{OUT}, & iteration > 1 \end{cases}$$
 (12)

4 Evaluation Environment

We have designed an experimental process to evaluate the effectiveness of interaction in a virtual environment afforded by the glove. The evaluation focuses on a 3D target acquisition task where the total time required to complete a fixed number of target acquisitions will be measured to assess the efficiency of the interaction. The robustness of the MARG orientation estimation method to magnetic distortions will be studied by involving targets whose acquisition require moving the glove in physical regions with and without known magnetic distortions.

To have available a basis for comparison, the subjects recruited for experimentation will be asked to complete the protocol with the virtual hand movements driven by two orientation algorithms (OA). One of them will be the well-known Kalman Filter [10, 22] (KF) method (OA = KF), which is available in an internal implementation within each MARG sensor. In other cases, the orientation estimates will be calculated with the GMVD μ k method, described in Sect. 3 (OA = GMVD μ k).

We will also seek to determine if the distance from the subject to the RGB-D camera has an impact on the efficiency of the interaction. To study this, each experimental subject will complete the protocol with the camera placed at D=D1=1 m and with the camera placed at D=D2=2 m, from the physical vertical plane that corresponds to the virtual plane in which the cubic virtual targets are placed. These variations of the setup are illustrated in Fig. 6.

4.1 Environment Setup

It is important that no large ferromagnetic materials be initially present in the space where the glove will be operated during the evaluation. This is necessary to avoid unknown distortions of the geomagnetic field. On the other hand, bars of M35 HSS high speed steel will be purposely placed near the right edge of the experimental area, to introduce a known magnetic distortion in the right edge of the experimental space. (These magnetic disrupters will be supported by a wooden pole in the neighborhood of the space where the magnetic distortion is desired, as described below.).

A large screen display will be provided for the visualization of the virtual scenario by the subject. This screen will be connected to the host computer to display the Unity® simulation to the subject. In this screen the subject will see the movement of the virtual hand in response to his/her physical hand movements.

A first wooden pole will be placed at the left side of the experiment area to provide the subjects with an initial physical landmark reference. The subjects will be told that it is expected that hand movements they will need to execute will take place to the right of this reference wooden pole.

A second wooden pole will be placed at the right side of the experiment area, symmetrically with respect to the left pole. In this case, subjects will be told that it is expected that hand movements they will need to execute will take place to the left of this reference wooden pole. In addition to serving as a physical reference, this right wooden pole will be used to support bars of M35 HSS high speed steel at the heights that will approximately match the virtual location of the cubes simulated in a column to the right of the virtual environment. This is for the purpose of introducing a known magnetic distortion that will affect the glove when the user attempts to acquire those targets ("4", "5" and "6" in Fig. 6).

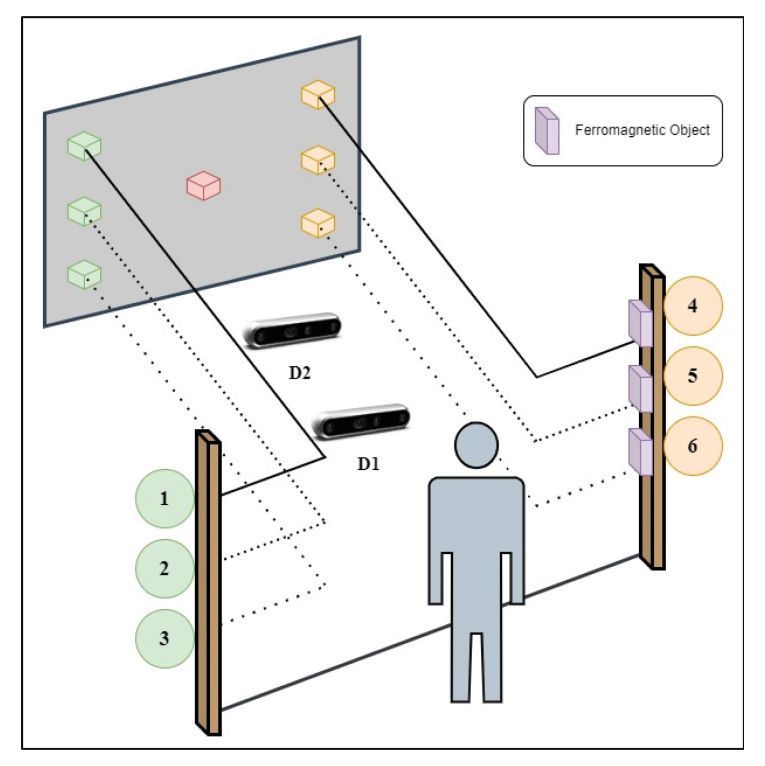


Fig. 6. Sketch showing the evaluation setup, including the location of the subject, the ferromagnetic materials, and the visualization screen, along with the 2 optional RGB-D camera locations.

4.2 Experiment Procedure

Each experimental subject will complete the evaluation protocol 4 times, with the orientation algorithm assigned at random to minimize ordering effects:

- 1. Two times with the RGB-D camera at 1 m (OA = KF followed by OA = GMVD μ k, or OA = GMVD μ k followed by OA = KF, assigned at random)
- 2. Two times with the RGB-D camera at 2 m (OA = KF followed by OA = GMVD μ k, or OA = GMVD μ k followed by OA = KF, assigned at random)

The subject will not be informed of the fact that there are two orientation algorithms being considered. The subject will not be told which algorithm is driving the simulation at any time. After providing informed consent, the subject will be asked to wear the glove and to adjust it comfortably in his/her hand.

The protocol requires the subject to acquire three (green) cubic targets located on the left side of the virtual scene (which will not require the glove to be operated in the magnetically distorted area). Then the user must acquire three (orange) cubic targets located on the right side of the virtual scene (which will require the glove to be operated in the magnetically distorted area). Specifically, the protocol will start by presenting the (red) home cube in the center of the scene. When the red cube is acquired by the subject, timer TIMER1 will start at 0, the red cube will disappear, and a first green cube ("1" in Fig. 6) will be presented in the virtual environment, to be acquired by the subject. When the first green cube is successfully acquired by the subject it will disappear, the time in TIMER1 will be recorded as T11, and the second green cube ("2" in Fig. 6, about 15 cm below "1", in the physical world) will be presented, for the subject to acquire it. When the second green cube is successfully acquired the time in TIMER1 will be recorded as T12, the second green cube will disappear and the third green cube ("3" in Fig. 6, about 15 cm below "2", in the physical world) will be shown, for the subject to acquire it. When the third green cube is successfully acquired the time in TIMER1 will be recorded as T13 and the third green cube will disappear.

When the subject has acquired all three of the green cubes, the home (red) cube will re-appear in the center of the scene, and the same process of sequential acquisition of three targets will be repeated for the orange cubes "4", "5" and "6" in Fig. 6, positioned on the right side of the virtual scene, symmetrically with respect to cubes "1", "2" and "3". A different timer TIMER2 will be used to record the times (T21, T22 and T23) at which the orange cubic targets are sequentially acquired.

The values of the recorded times (T11, T12, T13, T21, T22 and T23) will be the results from the experiment. Smaller values for these resulting times will indicate a lower difficulty in successfully acquiring the 3-D targets with the glove, allowing the comparison of performance with and without magnetic disturbances, and with respect to the camera distances (D1 or D2) and the orientation algorithms used (KF or GMVDµk).

5 Concluding Remarks

In this paper we have provided an outline of the development of our real-time hand tracking system based on a glove instrumented with MARG modules to estimate the orientation of the articulated segments of the hand.

Our approach relies on the real-time position tracking of just the wrist of the user, as provided by an RGB-D camera (Intel® RealSenseTM D455) through the Nuitrack Software Development Kit. The 3-D positions of the joints in each of the fingers of the hand are determined from that root wrist position by considering each of the fingers as a kinematic chain with segments of known lengths, and by using MARG sensor modules to obtain real-time orientation estimates of all the components in that kinematic chain: The metacarpal mass (modeled as a single rigid body), the proximal phalanx, and the middle phalanx. The orientation of the distal phalanx is not measured with a MARG module, and it is instead approximated by the relationship between the angle in the joint between the distal and the middle phalanges and the angle in the joint between the middle and the proximal phalanges [9].

Tracking the movements of the thumb requires the involvement of three MARG modules, since its metacarpal is articulated with respect to the metacarpal mass which includes the remaining four metacarpals. Therefore, MARG sensors were attached to all three of the articulated thumb segments: metacarpal, proximal phalanx and distal phalanx.

The fidelity with which the configuration of the physical gloved hand can be replicated in a corresponding virtual hand will be critically affected by the correctness of the orientation estimates generated by the algorithms that are used to process the output signals from the gyroscopes, accelerometers, and magnetometers in the MARG modules. For our prototype we use our GMVD μ k algorithm [19] which was developed with the aim of achieving resilient performance, even in areas where the geomagnetic field might be distorted by the presence of ferromagnetic objects. Section 3 of this paper provided an outline of the GMVD μ k method.

For the implementation of an initial proof-of-concept prototype we have created a glove in which only the thumb, the index finger and the middle finger are instrumented, which is sufficient to program the acquisition of virtual cubic targets.

In this paper we have also described the evaluation mechanism that we have designed for our interaction glove. It has been organized in such a way that it should allow us to study the impact of the distance between the glove user and the RGB-D camera. It has also been structured to explore the increased robustness of the GMVDµk orientation estimation with respect to the well-known Kalman Filter estimation method.

Acknowledgements. This work was supported by the US National Science Foundation grant CNS-1920182. Mr. Pontakorn Sonchan was supported by FIU's DYF fellowship.

Disclosure of Interests. The authors have no competing interests to declare that are relevant to the content of this article.

References

- Advanced Navigation: Inertial Measurement Unit (IMU) An Introduction. Tech Articles
 January 2024. https://www.advancednavigation.com/tech-articles/inertial-measurement-unit-imu-an-introduction/. 10 Jan 2024
- Aggarwal, P., Syed, Z., Noureldin, A., El-Sheimy, N.: MEMS-Based Integrated Navigation. Artech House GNSS Technology and Applications Series, vol. xiii, 197 p. Artech House, Boston, Mass.; London (2010)
- 3. Chen, Y., Wang, Q., Chen, H., Song, X., Tang, H., Tian, M.: An overview of augmented reality technology. J. Phys. Conf. Ser. 1237(2), 022082 (2019)
- de Vries, W.H.K., Veeger, H.E.J., Baten, C.T.M., van der Helm, F.C.T.: Magnetic distortion in motion labs, implications for validating inertial magnetic sensors. Gait Posture 29(4), 535–541 (2009)
- Dipietro, L., Sabatini, A.M., Dario, P.: A survey of glove-based systems and their applications. IEEE Trans. Syst. Man Cybern. Part C (Appl. Rev.) 38(4), 461–482 (2008)
- Foxlin, E.: Motion tracking requirements and technologies. In: Stanney, K.M. (ed.) Handbook of Virtual Environments, Design, Implementation, and Applications. Lawrence Earlbaum Associates (2002)
- Hanson, A.: Visualizing quaternions. Morgan Kaufmann Series in Interactive 3D Technology, vol. xxxi, 498 p. Morgan Kaufmann, San Francisco, Amsterdam, Boston. Elsevier Science distributor (2006)
- 8. Intel: Intel® RealSenseTM Product Family D400 Series Datasheet 2023 p. https://www.intelrealsense.com/download/21345/?tmsty=1697035582

- 9. Ip, H.H.S., Chan, C.S.: Dynamic simulation of human hand motion using an anatomically correct hierarchical approach. In: 1997 IEEE International Conference on Systems, Man, and Cybernetics. Computational Cybernetics and Simulation, vol. 1302, pp. 1307–1312. IEEE (1997)
- Kalman, R.E.: A new approach to linear filtering and prediction problems. J. Basic Eng. 82(1), 35–45 (1960)
- 11. Kortier, H.G., Sluiter, V.I., Roetenberg, D., Veltink, P.H.: Assessment of hand kinematics using inertial and magnetic sensors. J. Neuroeng. Rehabil. 11, 70 (2014)
- 12. Kuipers, J.B.: Quaternions and rotation sequences: a primer with applications to orbits, aerospace, and virtual reality, vol. xxii, 371 p. Princeton University Press, Princeton, N.J. (1999)
- López-Belmonte, J., Moreno-Guerrero, A.-J., López-Núñez, J.-A., Hinojo-Lucena, F.-J.: Augmented reality in education. A scientific mapping in web of science. Interact. Learn. Environ. 31(4), 1860–1874 (2023)
- 14. Madgwick, S.: An efficient orientation filter for inertial and inertial/magnetic sensor arrays. Report x-io Univ. Bristol (UK) **25**, 113–118 (2010)
- Mahony, R., Hamel, T., Pflimlin, J.M.: Complementary filter design on the special orthogonal group SO (3). In: 44th IEEE Conference on Decision and Control, pp. 1477–1484. IEEE (2005)
- Manuri, F., Sanna, A.: A survey on applications of augmented reality. ACSIJ Adv. Comput. Sci. Int. J. 5(1), 18–27 (2016)
- 17. Nuitrack: NUITRACK SDK, 10 January 2024. https://nuitrack.com/#api
- Ratchatanantakit, N., O-larnnithipong, N., Barreto, A., Tangnimitchok, S.: Consistency study of 3D magnetic vectors in an office environment for IMU-based hand tracking input development. In: Kurosu, M. (ed.) Human-Computer Interaction. Recognition and Interaction Technologies. LNCS, vol. 11567, pp. 377–387. Springer, Cham (2019). https://doi.org/10.1007/ 978-3-030-22643-5_29
- Sonchan, P., Ratchatanantakit, N., O-larnnithipong, N., Adjouadi, M., Barreto, A.: A self-contained approach to MEMS MARG orientation estimation for hand gesture tracking in magnetically distorted environments. In: Kurosu, M., Hashizume, A. (eds.) HCII 2023. LNCS, vol. 14011, pp. 585–602. Springer, Cham (2023). https://doi.org/10.1007/978-3-031-35596-7-38
- 20. Vince, J.: Quaternions for Computer Graphics, p. xiv, 140 p. Springer, London; New York (2011). https://doi.org/10.1007/978-0-85729-760-0
- 21. Woodman, O.J.: An introduction to inertial navigation. University of Cambridge (2007)
- 22. Xiaoping, Y., Aparicio, C., Bachmann, E.R., McGhee, R.B.: Implementation and experimental results of a quaternion-based Kalman filter for human body motion tracking. In: Proceedings of the 2005 IEEE International Conference on Robotics and Automation (2005)
- YostLabs: 3-Space Nano IC Product Description Page. Product Description for the 3-Space Nano IC MARG. https://yostlabs.com/product/3-space-nano/. Cited 5 Feb 2023